

Wind energy investigation of straight-bladed vertical axis wind turbine using computational analysis

Sukanta Roga^{1,*}

¹ Mechanical Engineering Department, Visvesvaraya National Institute of Technology, Nagpur-440010, Maharashtra, India

Abstract

Vertical axis wind turbines received renewed attention for increasing offshore wind energy harvesting and in urban environments. This turbine reflects a specific type of technology that generates electricity from wind, which is renewable sources of energy. This research explores the effect of blade profile modifications on the VAWT aerofoil NACA0012 and NACA2415. Analysis of the lift/drag coefficient and calculation of the average torque/self-starting potential of NACA0012 and NACA2415 for NACA0012, as this is a significantly better measure of the power generated at different pitch angles and comparison of both profiles. The dataset is created using Computational Fluid Dynamics (CFD) simulations, which were performed in ANSYS-Fluent. Various parameters, such as the number, thickness, and angle of attack of the Reynolds no. were investigated. The aerodynamics of the wind turbine blade is shown to increase the optimized form of the modified aerofoil.

Keywords: Aerofoil, NACA, Power, VAWT, Wind energy

Received on 30 September 2020, accepted on 15 October 2020, published on 27 October 2020

Copyright © 2020 Sukanta Roga et al., licensed to EAI. This is an open access article distributed under the terms of the [Creative Commons Attribution license](#), which permits unlimited use, distribution and reproduction in any medium so long as the original work is properly cited.

doi: 10.4108/eai.27-10-2020.166774

*Corresponding author. Email: rogasukanta@gmail.com

1. Introduction

Wind power is an important renewable source of energy, and in the past few years, it has become increasingly significant. The amount of wind power installed rises annually, and several nations have plans to make considerable wind power investments in the near future. Many studies have been undertaken to design, simulate, and characterize wind performance, to encourage the market acceptance of wind power by offering tools to support and improve the research and development sectors. Wind energy investments for the 27 EU member states are expected to increase by close to EUR 20 billion in the next 20 years, accounting for 60 % of this offshore investment by 2030. In the past, the government has set itself the 2010 wind power target of 3750GW for Portugal alone. The overall installed capacity of the 3750MW was already about 25 %. However, the latest government objectives for the wind sector have recently raised this value to 5100MW. A wind turbine is a mechanical device that converts wind energy into usable mechanical energy for electricity generation. The Darrieus wind turbine is a type of wind turbine of the vertical axis wind turbine (VAWT) used to produce power from wind

power. Several wind turbines with direct blades are closely related to this. This turbine design was patented by a French aeronautical engineer, Georges Jean Marie Darrieus [1].

The protection and self-starting of the Darrieus turbine from extremes of wind are essential. During the severe wind conditions, wind turbine safety is challenging to minimize by adding an engine and generator control unit. VAWT provides various advantages such as the wind direction independence, no additional wind control systems are required, and the ability to operate in a wide range of wind conditions (turbulence level, wind speed). From a design consideration point of view, few parameters are required to be considered while designing the wind turbine, such as swept area, power and power coefficient, tip speed ratio, blade chord, number of blades, solidity, etc. These wind turbines rotate to produce electricity where the blades have airfoil shapes. Because of these shapes, these blades get lift force, gives it rotational energy [2].

1.1. Theoretical background

The amount of absorbed wind power, P can be found from

$$P = 1/2 C_p \rho A v^3 \quad (1)$$

where,

C_p is the coefficient of power,

ρ is the air density,

A is the swept area of the turbine, and v is the speed of the wind.

The power coefficient represents the aerodynamic efficiency of the wind turbine and also is a tip speed ratio function, λ which is defined as,

$$\lambda = \omega R/v \quad (2)$$

where,

ω is the rotational frequency of the turbine,

R is the radius of the turbine, and

v is the speed of the wind.

The solidity, σ states a relation between the blade area and the turbine swept area and has different definitions for different types of turbines; for a VAWT it is defined as,

$$\sigma = Bc/R \quad (3)$$

where,

B is the number of blades present,

c is the length of the chord, and

R is the radius of the turbine.

1.2. Airfoil profile designation

The National Aeronautical Consultative Committee (NACA) aerofoils are the arrangement of numbers after NACA. The numerical code can be used in aerofoil mathematical declarations to generate and calculate the aerofoil's cross-section. Using scientific comparisons that depict the midline (geometric centric line) camber of the aerofoil region and its thickness transport along the length. NACA aviation system was developed, the 4-digit, 5-digit, and adjusted 4 to 5 digits. Subsequently, like the 6-series, ambiguous types using hypothetical techniques were inferred. Apart from their past association with established types and experimental modifications to these types, the aerofoils design was a little arbitrary until the NACA joined the arrangements. Distinctive profiles of the NACA aerofoil are shown below:

1.2.1. Four-digit series

The NACA 4-digit is described with the following:

- In the first digit, the maximum camber is given as a percentage of the total chord length
- Second digit allows for tens of the chords percentage to separate the full camber from the leading edge.
- Last Two digits define the airfoil as the chord's maximum thickness chord percentage.

The NACA2412 airfoil, has the largest camber of 2%, its leading-edge position is 40% chord, and its overall chord thickness is 12%. The aerofoil NACA0015 is symmetrical; the 00 means it does not have a camber. The 15 reveals that the airfoil has a chord-length ratio of 15% thickness.

1.3. Blade profiles Selection

1.3.1. NACA0012

- It is asymmetrical with 0% camber at 0% chord.
- Maximum thickness = 12% at 30% of the chord length.
- This airfoil has been found to have a low starting torque requirement for rotation of the turbine.

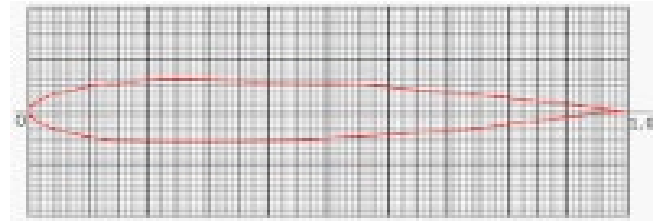


Figure 1. NACA0012 profile

1.3.2. NACA2415

- It is an asymmetrical airfoil with camber.
- Maximum thickness = 15% at 29.5% of the chord length.
- Maximum camber = 2% at 39.6% chord length.

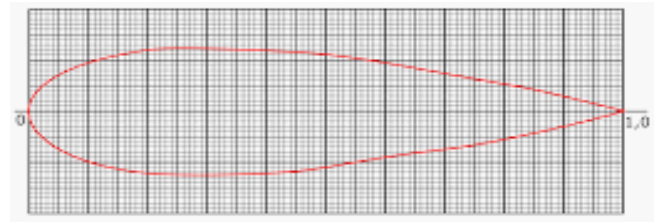


Figure 2. NACA2415 profile

1.3.3. Selection of NACA0012, NACA2415 based on the following

- The literature survey on the self-starting criteria for selection of airfoils like, NACA0012 and NACA2415.
- The considerations of self-starting capability as done by the study of several symmetrical blade profiles, the thicker blades show a better performance of self-start.

2. Literature review

2.1. Major findings based on Darrieus turbine

The behavior was analyzed of the flow around a VAWT blade airfoil when it is stopped to develop new blade profiles capable of offering the lift type VAWT the ability to self-start. One of the articles covered the study of curved and straight-bladed VAWT, its comparison, advantages, and disadvantages VAWT have both curved and straight blades [4]. The actual experiment is carried out at the Bialystok University of Technology (BUT) on an open environment to get power output and taken reading of power output for three years (2015 to 2018) with variable wind speed. H-Darrieus three-blade VAWT with 3.5 m blade

diameter and 3m height is used for 5kW power generation capacity. CML software for the impact assessment method is used to study the life cycle assessment [5].

The wind energy from vehicles running on the highway can be effectively utilized and converted into electrical energy which can be stored in a battery and used for small-scale purposes like street lighting, traffic light, traffic cameras, railway crossing, etc. This design concept is sustainable and environmentally friendly. In the future, it must help to overcome the energy crisis in the World. It compared aerodynamic blade loads and wake velocity profiles computed by CFD with the experiments for the vertical axis wind turbine. The CFD analysis was compared with experimental findings in aerodynamic loads. The results are suitable for all turbulence models used. According to experimental results for the azimuth spectrum, all CFD and VTM tests are between 220 and 360 degrees, respectively [6].

Site selection and turbine install are made manually. The 3D ultrasonic anemometer is used for measuring the wind speed at 5.3m mast height. The reading is taken for one year at different z/h ratio. This experiment gives the turbulence power spectral density for all three directions that are longitudinal, lateral, and vertical. For this calculation, three models are used by Von Karman, Kaimal, and measurement value from which Kaimal model gives the best result. To investigate the best model/profile, this study used the degree of misfit function to measure power spectra. The Von Karman spectra predicted all wind components are low than the Kaimal. It is observed that the Kaimal model gives the best predictions to install the small wind turbine on the rooftop at that particular site only [7].

It is recognized that Darrieus turbines have the benefit of operating at low wind speed and the vertical axis turbines are aerodynamically small compared with those with a horizontal axis. This work analyzed the force and its derivative in drag forces. It tested for the limit for Lenz turbine blade with a wind speed of between 6-10 m/s, which is possible for different blade types. This research was carried out using ANSYS-Fluent. There are two main types of investigation: theoretical and experimental methods, which enable SB-VAWT to be found as a sort of Darrieus VAWT. Even with the development of efficient, less energy-consuming devices, the theoretical method includes aerodynamic computational and numerical simulation models and the regular need for electricity. The proposed VAWT model is a vital renewable energy source for highways [8].

The open terrain with wind speed ranges from 10-25 m/s are valid for the current standard IEC 61400-2 design. The extreme wind condition models and standard wind condition turbulence model do not capture small wind speed from the urban area condition. This review mainly focused on the characteristics of wind flow in the urban area. The parameters like atmospheric stability, hub-height, etc. influence the operating conditions. This work also shows that the spherical shape roof improves the 50% more performance than other rooftop turbines. The turbulence can be minimum at 50% above the building height. To

understand the performance, power output, and loading capacity of a small wind turbine, the small wind turbine installation inflow in the built environment, and on understanding to what extent the international standard design of small wind turbine is done for installation in built environment [9].

2.2. Effect of a blade profile, the Reynolds number, and the solidity on the performance of a straight-bladed VAWT Sung-Cheoul Roh and Seung-Hee Kang

2.2.1. Effect of blade profile

The results confirmed the direct impact of the blade profile on turbine performance. The symmetrical high-digit NACA profile offers higher energy in the low Tip Speed Ratio (TSR), λ , (TSR<3) range than the symmetric low digit balanced NACA profile. The low-digit symmetrical NACA has greater control over the high-digit symmetric NACA profile in the high TSR (TSR>5). The four-digit balanced NACA airfoil profile has been selected to determine the effects of the blade profile for a straight = type Darrieus VAWT, and the turbine performance of different blade profiles has been evaluated at Reynolds no=360,000 and $\sigma = 0.0833$ [10].

2.2.1.1. Effect of Reynolds number

Reynolds is a significant factor in the increase of speed power output ($1 < \text{TSR} < 12$), but with Reynolds introduction, the additional power generation is irrelevant.

2.2.1.2. Effect of solidity

The power production at Reynolds no of 360,000 appears to be increasing in solidity to $\mu = 0.25$, then seems to be decreased by further increased strength from $\mu = 0.25$ to 0.5 and also decreased blade velocities [11] with a variation in solidity range

The performance of the peak between the Darrieus VAWT straight type and the Darrieus VAWT eggbeater type is substantially different

2.2.2. Pitch angle control for a small-scale Darrieus VAWT with straight blades

2.2.2.1. Effect of Pitch control on the performance of turbine

Larger amplitude pitch at low TSR reduces the attacking angle and improves rotor performance. In comparison, broad pitches will deteriorate VAWT output on high TSR's and vice versa.

The experimental results of researchers show that the variable pitch had a coefficient of 25-30 % higher than the set blade ($\beta = 0$ degree). A variable pitch technique is applied by changing the angle of attachment (α) to improve the performance of the VAWTs. A variable pitch control

system has two types of pitch systems. i.e., active and passive.

Active: Pitch control mechanisms like pushrods, cams, or servomotors in a dynamic control system were created with a view to continuous modification of the pitch control.

Passive: The blade can move/pitch around its axis near the front edge in a passive variable pitch control system. Theoretically, the start torque and performance of VAWT can significantly improve the passive control system.

It is required to use a variable TSR control system to decrease attack angle and improve starting torque to improve startups autonomy [12].

2.3. Self-starting capability of a Darrieus turbine

The study described here aims to examine their initial performance by developing, validating, and establishing the parameters that govern auto-starting capabilities. The use of the widely used and documented, symmetric turbine blade profile NACA0012 is used to present a case study. It has been demonstrated that a slightly loaded three-bladed rotor can always start on its own under constant wind conditions, while the start of a two-bladed unit will depend on its initial starting orientation.

According to Ebert and Wood: Self-starting process is defined as have been completed when significant power extraction commenced.

2.4. Numerical study of blade thickness and camber effects on vertical axis wind turbines

The findings of a two-dimensional measurement analysis on the impact of the rotor blades thickness and camber on the output of a 5kW vertical wind turbine axis. The validity of a pitching airfield with a dynamic stop phenomenon is given by comparison to experimental evidence.

The turbines output is mapped to establish how and mainly why the turbine efficiency varies with thickness and camber as much as it does for different tip speed ratios. The NACA0012, NACA0022, NACA5522, and LS0421 rotor blades were chosen. The NACA0012 profile was carried out with the highest overall performance of 50 % in the range of tip speed ratios tested.

The overall output of the vertical axes turbine can be improved by slightly cambered aerofoils, e.g., LS0421, while a 5% camber can lead to the poor performance of the cambered blades. With a maximum C_p of 0.40 at $1/4$ 3.5, the LS0421 is the best performance of the trucks tested. The blades produce higher torque rates in the upwind and downwind regions by a camber along the blade's path, which is also found to have energy, mainly in the upwind area, with inverted cambered profiles. The validity of a series of turbulence models for VAWT simulations was evaluated with a pitching aerofoil test. The SST k model was shown to be a perfect agreement in both strength and flow predictions. The SST k-epsilon is the most suitable turbulence model for use with a dynamic stall phenomenon in unstable aerofoil movement. 2D simulations of VAWT

blade aerofoil thickness and camber shift output effects were performed.

The findings show that the thinner blade with maximum C_p up to 0.50 in favor of the NACA0012 by $1/43.5$ for the two aerospace symmetries tested. The NACA0012 aerofoil performs better than the NACA0022 throughout the entire range of tests. Slightly cambered aerofoils like the LS0421 profile can improve VAWT's overall performance, whereas a 5% camber is unfavorable with NACA5522. In general, the cambered NACA5522, in particular in high-regions, is less than the symmetrical NACA0022. The LS0421 is the best with a maximum C_p of 0.40 on $1/4$, 3.5 of the more thick blades tested. A camber along the blade path contributes to high torque rates in both the upwind as well as the downwind. However, only upwind power is generated by inverted cambered profiles. The NACA0012 provided the best total aerodynamic performance for power extraction between the different blade profile investigation. The CFD flows visualizations, accompanied by a non-traditional debate on flow physics guide how to conduct VAWT efficiency analyses [12].

3. Methodology

The methodology process starts with analyzing and studying different research work. Additional research articles have been reviewed on various topics related to blade design aerodynamics and parameters. It has been decided to investigate blade profiles with ANSYS-Fluent software platform, which is widely used in the aerodynamic and automobile industries. The flow chart given below shows the primary analysis sequence used here.

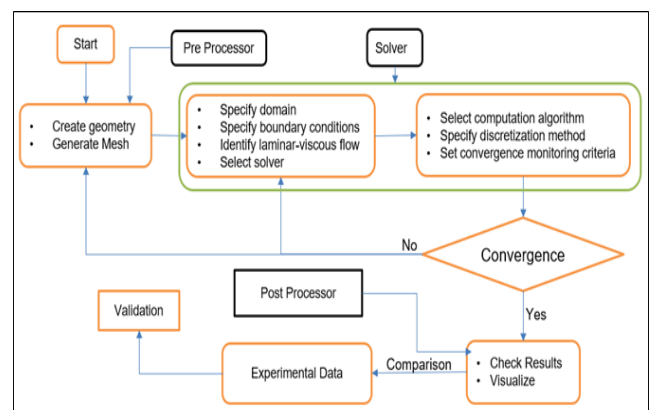


Figure 3. Methodology flow chart

3.1. Computational geometry

Computational domains are prepared to study around the vertical axis wind turbine profile. Different surfaces and edges have been generated for geometry preparation, which has been adequately arranged [13]. Other edges and surfaces have been named inlet, outlet, upper wall, a bottom wall, and airfoil. Also, surfaces have been designated as fixed domains, and the fixed domain is that rectangular geometry where a circular area is not present. For generating proper

surfaces, the Boolean function of ANSYS-Fluent from the concept is used. It has been prepared in Workbench.

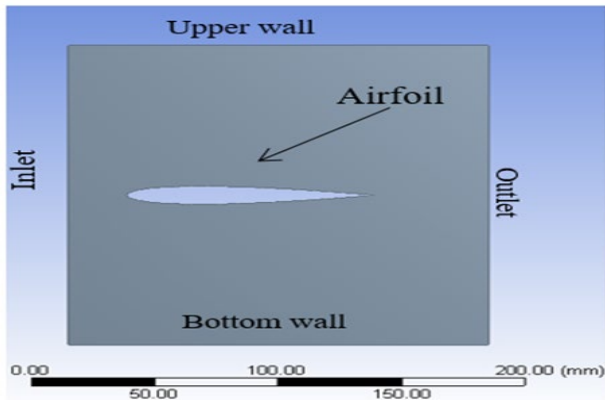


Figure 4. Geometry of NACA0012 at $\alpha=0^\circ$

3.2. Meshing

For mesh distribution, several features of meshing in ANSYS-Fluent is used. For body sizing, the element size as 0.5 mm is provided, which is enough good compare to 180 mm. then edge sizing is given on the inlet and outlet wall. The number of divisions selected was 200, which was enough for edge sizing. Meshing is done according to these parameters by selecting appropriate edges and reference surfaces.

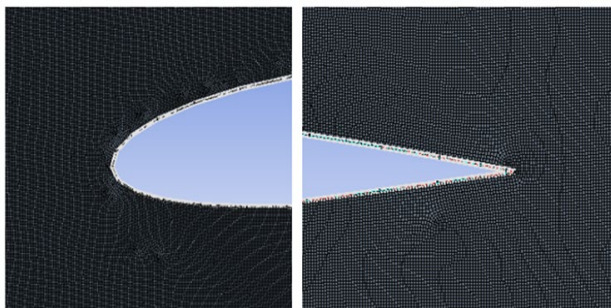


Figure 5. Meshed geometry near airfoil edges (Zoom view)

Meshing parameters have been decided according to the accuracy and precision required in the results. Around edges, the coarse mesh is necessary to get more accurate results. Meshing is started by naming the section first and then specifying different meshing parameters which is shown in figure 5.

3.3. Setup

The pressure and absolute velocities transient flow is considered, and it is planar for the geometry, flow is viscous and compressible. Wind velocity is considered as 5m/s for initial calculations. The viscosity is considered as 1.18 kg/m³. Temperature is assumed to be atmospheric, and the value of kinematic viscosity has been considered according to it.

The k-epsilon model has been considered, and solving equations has also selected enhanced wall function for near-wall treatment. For the inlet, boundary conditions are given as inlet velocity 5 m/s. Similarly, the conditions are given for the outlet, the upper wall, and the bottom wall. Reference values have been taken as default.

3.4. Solution

For solution controls, the following conditions are considered.

Turbulent kinetic energy, k

$$\frac{\partial(\rho k)}{\partial t} + \frac{\partial(\rho k u_i)}{\partial x_i} = \frac{\partial}{\partial x_j} \left[\frac{\mu_t}{\sigma_k} \frac{\partial k}{\partial x_j} \right] + 2\mu_t E_{ij} E_{ij} - \rho \epsilon \quad (4)$$

For dissipation,

$$\frac{\partial(\rho \epsilon)}{\partial t} + \frac{\partial(\rho \epsilon u_i)}{\partial x_i} = \frac{\partial}{\partial x_j} \left[\frac{\mu_t}{\sigma_\epsilon} \frac{\partial \epsilon}{\partial x_j} \right] + C_{1\epsilon} \frac{\epsilon}{k} 2\mu_t E_{ij} E_{ij} - C_{2\epsilon} \rho \frac{\epsilon^2}{k} \quad (5)$$

The rate of change of k or ϵ + Transport of k or ϵ by convection = Transport of k or ϵ by diffusion + Rate of production of k or ϵ - Rate of the destruction of k [13]. In monitors, parameters for Cl and Cd are the coefficient of lift and drag coefficient.

3.5. Model validation

Figure 6 presented the pressure variation of NACA0012 aerofoil.

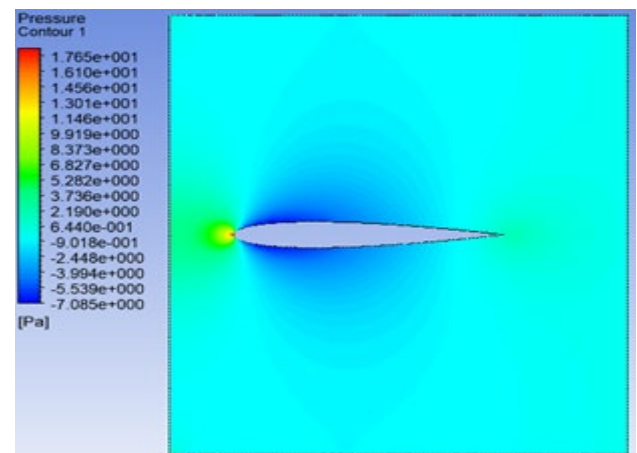


Figure 6. Pressure variation of NACA0012

4. Results and discussion

4.1 Pressure and velocity variation

Analysis of two blade profiles, i.e., NACA0012 and NACA2415 on various parameters starting with Reynolds number. Reynolds number considered here is 50000 and 100000. The coefficient of lift and drag were studied for both the Reynolds numbers. The analysis begins with essential pressure and velocity variation at $\alpha = 0^\circ$.

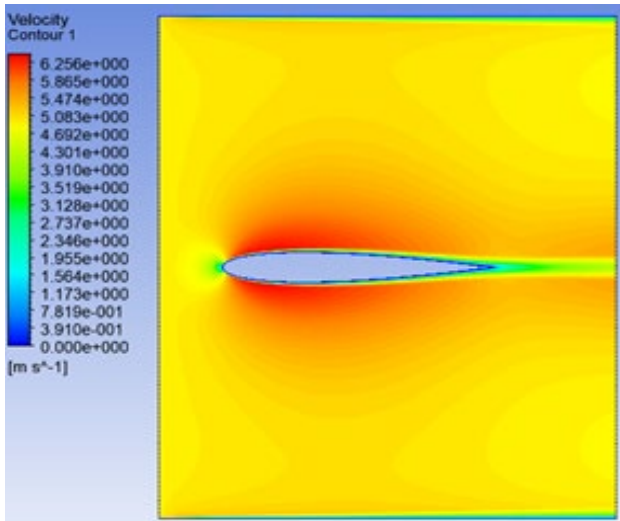


Figure 7. Velocity variation of NACA0012

From the pressure variation on NACA2415 profile, it is investigated that both the blade profiles show similar kinds of behaviors. The higher pressure values at the leading edge that is the impact point, red color shows a higher value of pressure, where blue color is indicating the least value of pressure. Near the side edges, the pressure is reduced for both the profiles, and this variation in pressure helps in lift force, and those are presented in figures 6 to 9.

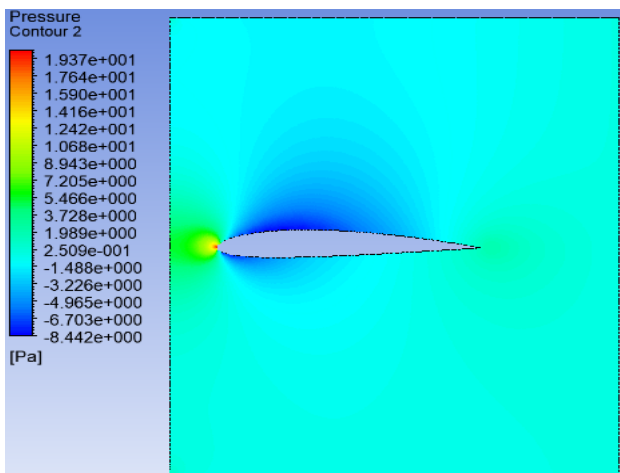


Figure 8. Pressure variation of NACA2415

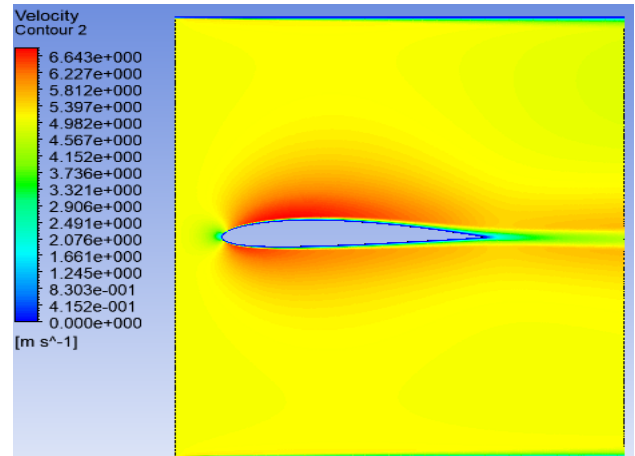


Figure 9. Velocity variation of NACA2415

When the velocity is considered, again, similar behavior is shown initially by both blade profiles. At the impact point, the value of velocity is reduced, as seen from the figure, whereas near side edges, velocities of rates increase, resulting in lift force.

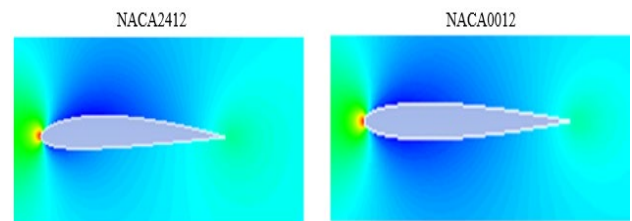


Figure 10. Comparison of pressure variation

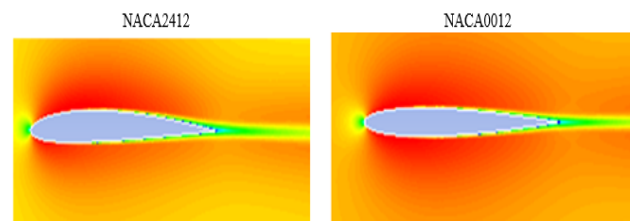


Figure 11. Comparison of velocity variation

4.2. Reynolds number study

Pressure and velocity variations are appropriately compared here in figures 10 and 11. The analysis was with two different Reynolds numbers cases, which are 50000 and 100000. The following results are observed: At 50000 Reynolds number, lift and drag coefficients are studied. For $\alpha=0^\circ$, the lift coefficient is zero for the symmetric blade that is NACA0012 whereas for asymmetric that is NACA2415 is 0.0354 turning higher lift to drag coefficient. Similarly, for 100000 Reynolds number, analysis has been done. The lift coefficient is 0 for NACA0012, and the value of the lift coefficient is 0.01918 for asymmetric profile design, which is presented in figures 12 and 13.

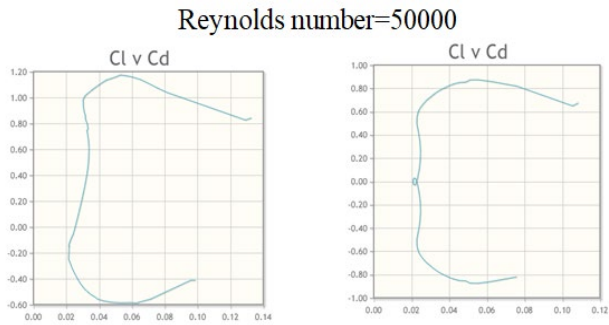


Figure 12. Coefficient of lift vs drag

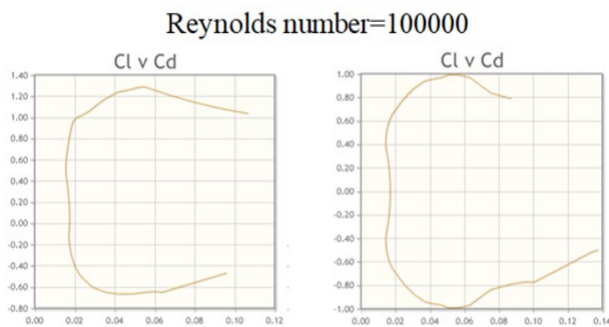
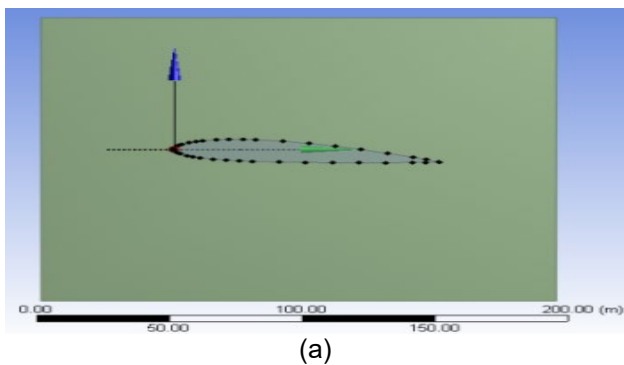


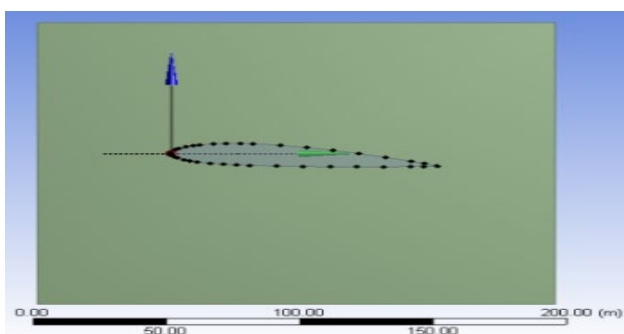
Figure 13. Coefficient of lift vs drag

4.3. Pitch angle variation

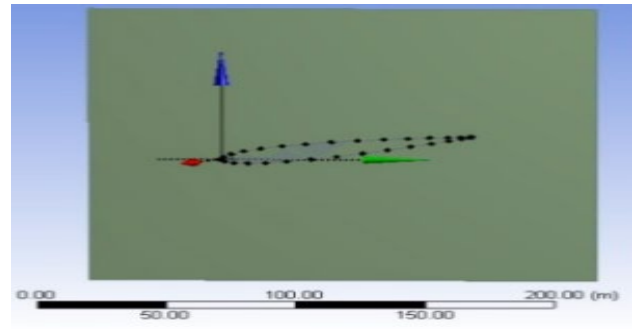
For the second part, the pitch angle is diverse in the range of -12.5 degrees to 10 degrees. The coefficients of lift and drag are found out at different angles. Reynolds number is considered as 100000, and different pitch angles are considered while analyzing.



(a)



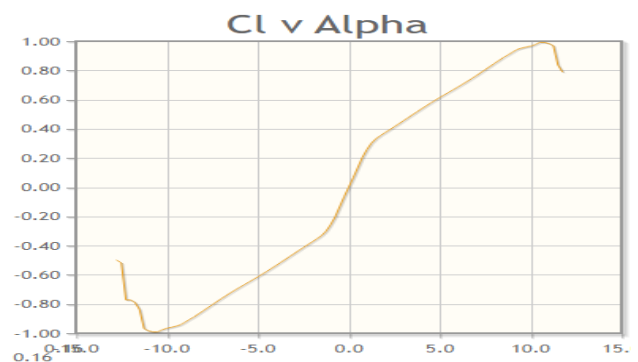
(b)



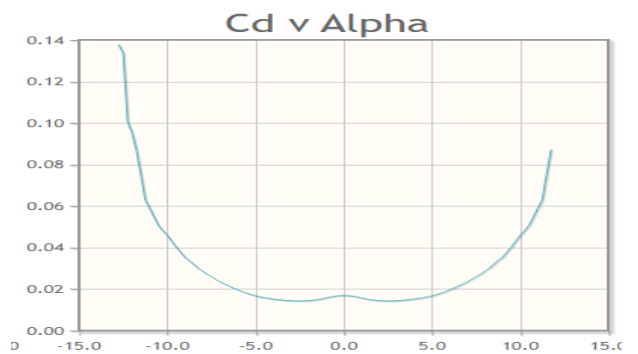
(c)

Figure 14. Geometries of NACA0012 (a) $\alpha=0^\circ$, (b) $\alpha = -5^\circ$, and (c) NACA2415 at $\alpha = 5^\circ$

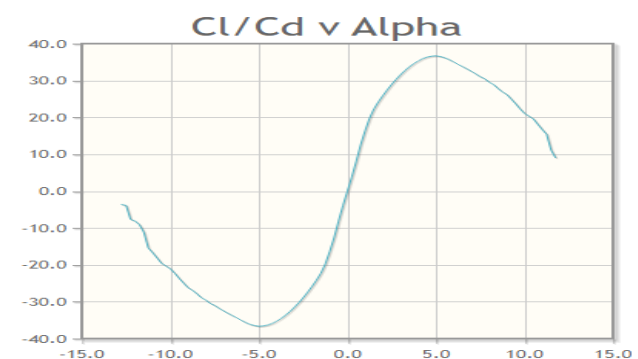
4.3.1. For NACA0012



(a)



(b)



(c)

Figure 15. Relations of coefficients and alpha (a) Cl v alpha, (a) Cd v alpha and (a) Cl/Cd v alpha for NACA0012

For the range of pitch angles and Reynolds number 100000, lift, drag, and lift coefficient is studied. After analysis, the lift coefficient value to drag is highest at $\alpha = -5^\circ$ value of the lift coefficient as 0.6141 and for drag as 0.01674, which is presented in figure 15.

4.3.2. For NACA2415

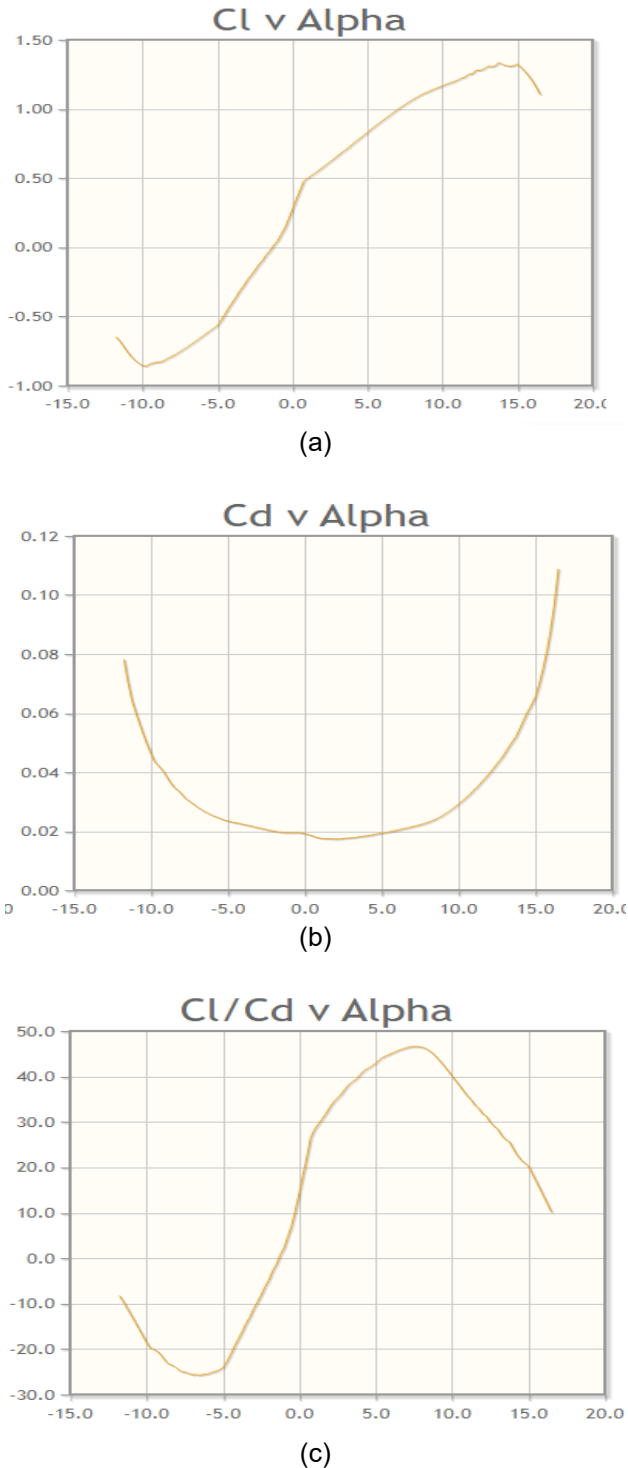


Figure 16. Relations of coefficients and alpha (a) Cl v alpha, (a) Cd v alpha and (a) Cl/Cd v alpha for NACA2415

Again similarly, for the range of pitch angles and Reynolds number of 100000, coefficient of lift, drag, and lift to drag are studied. After analysis, the lift coefficient's value to drag is highest at $\alpha=8.5^\circ$ value of the coefficient of lift as 1.096 and for drag as 0.02398.

It is observed that higher values of lift to drag coefficients are getting for asymmetric that is NACA2415 at Reynolds number 100000, which is presented in figure 16.

5. Conclusions

The conclusion has been inferred from two studies that are Reynolds number and Pitch angle variation. The parameters and factors considered here are all discussed in detail. A pressure and velocity variation study has been done, as well.

5.1. Reynolds number

Studying lift and drag coefficient at two Reynolds number that is 50000 and 100000 concluded that values of coefficients at higher Reynolds numbers are higher, resulting in less starting torque required, so the selection of Reynolds number as 100000 while designing rotor will be an efficient decision in performance point of view.

Comparing these blade profiles that are NACA0012 and NACA2415, the asymmetric blade profile that is NACA2415 gives higher values in the lift to drag coefficient, so while designing vertical axis wind rotor, among these two, asymmetric blade profile will be preferable inefficiency point of view. Higher values of lift coefficient are generated in the case of NACA2415 analysis.

5.2. Pitch angle variation

The range of pitch angles has been studied for understanding the effect of pitch angle on the performance of airfoils and their efficiency for self-starting capability. Self-starting capability's primary requirement is the least torque initially required, so ultimately higher values of lift and lower values of drag coefficient are needed.

As from previous analysis, 100000 Reynolds number is taken for further research. For NACA0012, the highest value is achieved at $\alpha=5^\circ$, it will be efficient from the design viewpoint, and for NACA2415 value is 8.5° , which parameters have been considered from the designing approach of VAWT.

6. Future scope

From the analysis, it is understood that asymmetric blade profiles are better than symmetric blade profiles in some aspects. More designs can be studied and analyzed on different Reynolds number values and other parameters like the blade thickness, the blades material, etc. Also, the number of blades can be varied according to application. Efficiency can self-starting can be studied and analyzed.

Acknowledgment

The author expresses his sincere gratitude to Computational Fluid Dynamics Lab Coordinator and the Director, VNIT Nagpur for their constant support.

References

1. R. B. Sholapurkar and Y. S. Mahajan, "Review of Wind Energy Development and Policy in India," *Energy Technology and Policy; Policy*, vol. 2, no. 1, pp. 122–132, 2015.
2. S. Joo, H. Choi and J. Lee, "Aerodynamic characteristics of two-bladed H-Darrieus at various solidities and rotating speeds," *Energy*, vol. 90, pp. 439–451, 2015.
3. G. Abdalrahman, W. Melek, and F.-S. Lien, "Pitch angle control for a small-scale Darrieus vertical axis wind turbine with straight blades (H-Type VAWT)," *Renewable Energy*, vol. 114, pp. 1353–1362, 2017.
4. S. Karan, Y. Arpit, Z. Yuvraj, P. Siddharth and D. Sapariya, "Design, Analysis and Fabrication of Vertical Axis Wind Turbine," *International J for Scientific Research and Development*, vol. 6, pp. 91-3, 2018.
5. V. Kouloumpis, R. A. Sobolewski and X. Yan, "Performance and life cycle assessment of a small scale vertical axis wind turbine," *Journal of Cleaner Production*, vol. 247, p. 119520, 2020.
6. Y. Li, "Straight-Bladed Vertical Axis Wind Turbines: History, Performance, and Applications," *Rotating Machinery*, 2020.
7. A. B. Tabrizi, J. Whale, T. Lyons and T. Urmee, "Extent to which international wind turbine design standard, IEC61400-2 is valid for a rooftop wind installation," *Journal of Wind Engineering and Industrial Aerodynamics*, vol. 139, pp. 50–61, 2015.
8. S. Karhadkar, S. Kanetkar, N. Pawar and H. Mistry, "CFD Analysis For Computing Drag Force On Various Types of Blades for Vertical Axis Wind Turbine," *International Research Journal of Engineering and Technology*, vol. 5, no. 1, pp. 1110-1112, 2018.
9. A. Kc, J. Whale and T. Urmee, "Urban wind conditions and small wind turbines in the built environment: A review," *Renewable Energy*, vol. 131, pp. 268–283, 2019.
10. R. Dominy, P. Lunt, A. Bickerdyke and J. Dominy, "Self-starting capability of a Darrieus turbine," *Proceedings of the Institution of Mechanical Engineers, Part A: Journal of Power and Energy*, vol. 221, no. 1, pp. 111–120, 2007.
11. N. C. Batista, R. Melicio, J. C. O. Marias and J. P. S. Catalao, "Self-start evaluation in lift-type vertical axis wind turbines: Methodology and computational tool applied to asymmetrical airfoils," *2011 International Conference on Power Engineering, Energy and Electrical Drives*, 2011.
12. P. Nagare, A. Nair, R. Shettigar, P. Kale and P. Nambiar, "Vertical axis wind turbine," *2015 International Conference on Technologies for Sustainable Development (ICTSD)*, 2015.
13. A. Sharma, "Computational Fluid Dynamics: Physical Law based Finite Volume Method," *Introduction to Computational Fluid Dynamics*, pp. 251–269, 2016.